



## Comparison of conventional and through glass portable chest computed radiography: A Phantom study

Kingkarn Aphiwatthanasumet

Department of Radiological Technology, Faculty of Allied Health Sciences, Naresuan University, Phitsanulok Province, Thailand

### ARTICLE INFO

#### Article history:

Received 28 November 2021

Accepted as revised 4 December 2021

Available online 31 January 2022

#### Keywords:

Portable chest radiography, through glass, glass attenuation, COVID-19 pneumonia, scatter radiation

### ABSTRACT

**Background:** Since the outbreak of COVID-19, modified hospital unit or area for chest radiography of positive cases have become necessary. To date, relatively few studies have been investigated on the effects of portable chest radiography through glass barrier.

**Objectives:** Our goal was to evaluate exposure technique and radiation dose between conventional and through glass portable chest computed radiography.

**Materials and methods:** Experiments using an anthropomorphic phantom were performed for acquired portable chest PA radiography at SID 180 cm with glass door being open and closed. The EI and DI values were optimized to provide the appropriate exposure technique for glass barrier. Entrance surface air kerma and scatter survey were made to assess the radiation dose both inside and outside the room. Finally, HVL measurement of primary X-ray beam and after transmission through glass were determined.

**Results:** Based on the fixed kVp and mAs technique, the EI value with glass barrier was less than the EI without the glass. Imaging through glass barrier showed the average EI reduction of 10.4% for Carestream and 37% for Konica. The average entrance surface air kerma reduction was 56.6% over a range of 90-120 kVp. The appropriate exposure technique for conventional portable chest PA using computed radiography was 100 kVp 2.5 mAs. With the same kVp setting, doubling the mAs is required for imaging through glass barrier to produce good diagnostic image quality (100 kVp and 4.0 mAs). The acceptable EI and DI ranges for CR used were EI=1742, DI=-0.02 (without glass) and EI=1795, DI=0.11 (with glass) for Carestream and EI=352, DI=-0.03 (without glass) and EI=373, DI=0.22 (with glass) for Konica respectively. The primary beam after transmission through the glass thickness 5 mm was 36%. The measured scatter of inside room compared to outside was very low at 1-2 meters. Increasing od HVL from 3.9 to 6.1 mm Al indicates the effect of beam hardening by glass.

**Conclusion:** These experiments confirmed that through glass portable chest computed radiography are feasible and safe. The findings of this study have several practical implications which minimizes risk to radiographers during their work.

\* **Corresponding author.**

**Author's Address:** Department of Radiological Technology,  
Faculty of Allied Health Sciences, Naresuan University, Phitsanulok  
Province, Thailand.

\*\* **E-mail address:** [kingkarna@nu.ac.th](mailto:kingkarna@nu.ac.th)

doi: 10.12982/JAMS.2022.010

E-ISSN: 2539-6056

## Introduction

Chest radiography plays a key role in monitoring disease progression in patients infected with coronavirus disease 2019 (COVID-19).<sup>1,2</sup> In the first week of illness, patients with no symptom or mild symptom may have normal baseline chest radiograph while the patients with moderate or severe symptom have abnormal finding on baseline chest radiograph. Imaging features of COVID-19 pneumonia on chest radiograph has a pattern of increased density within the lung. Typical radiographic features include ground glass opacities, peripheral opacities, consolidation, multifocal and diffuse air space opacities.<sup>3-5</sup> The most common chest radiographic finding of COVID-19 pneumonia is bilateral multifocal air space opacities or (consolidation) in the peripheral and lower lung zones. Additional follow-up chest X-ray of all patients are preferred due to evidence of COVID-19 on chest radiograph help understanding how individual disease progress and worsening clinical status.

Radiographers worldwide have reported an increase in workload during the pandemic.<sup>6</sup> At the first wave of COVID-19, the major problem are limited availability of vaccine for frontline workers and a shortage of personal protective equipment (PPE). Likewise, lack of experience in working with infectious patients showed that medical staffs had been infected.<sup>7</sup> One way to prevent the spread of infections is to educate them regarding infection control practices. Modified hospital unit, isolation room, or area for chest radiography of positive cases have become necessary.

Many hospitals applied portable chest radiography through glass technique (TG-CXR) of the confirmed positive patients to limit staffs direct contact with patients.<sup>8</sup> This technique can reduce the risk of infection due to keep the patients in place and limit transmission of the virus.<sup>9-11</sup> The glass door attenuates and filters some X-ray photon in the beam. At higher X-ray beam energy, transmission of primary beam is increased and become more penetrating. Optimization exposure technique is one that provide the lowest possible patient dose for sufficient image quality. A high kilovoltage peak (kVp) and low miliampere-seconds (mAs) are needed to produce the posteroanterior chest radiography (CXR). These techniques reduce radiation dose to patient while preserving good contrast detectability with infectious lung disease. However, there have been no controlled studies which compare the radiation exposure at the detector and radiation dose between conventional and through glass portable chest computed radiography. Here, we became interested in the idea of distance imaging and modified through glass portable radiography. The aim of this study was to evaluate exposure technique and radiation dose between conventional and through glass portable chest computed radiography.

## Materials and methods

An anthropomorphic thorax phantom of an adult male (Model RS-111 Opaque, United States) was used to simulate the clinical experiments. The phantom positioned for an erect postero-anterior (PA) chest radiography. A Toshiba mobile x-ray model IME-100L was set up outside the isolation room at a SID of 180 cm (Figure 1). The image receptors

were all computed radiography system, one by Carestream (DirectView Vita CR) and one by Konica Minolta (Regius Sigma II). The imaging plate had an image capture area of 35x43 cm. The quality control (QC) tests of equipment were monitored in accordance with the recommendation of AAPM Report No. 74 and 93 before reporting the measurement results.<sup>12,13</sup> We performed portable chest radiography by setting up equipment with door open (conventional technique) and through the glass door of an isolation room (TG-CXR technique). The glass door we use was a regular glass in standard thickness of 5 mm. The experiment was tested with door open and with door closed (through glass imaging) as shown in Figure 2. All radiation measurements were obtained with a RaySafe X2 radiation meter (Unfors RaySafe, Sweden). We measured at selected point as described in a previous work.<sup>9,10</sup> Dosimeter was positioned at the center of the thorax phantom to measure radiation dose. Entrance surface air kerma (ESAK) in microgray ( $\mu\text{Gy}$ ) were made and normalized to mAs (by dividing mAs to give  $\mu\text{Gy}/\text{mAs}$ ). In the presence of scatter radiation inside the room, the X2 survey probe positioned in the forward, side, and backscatter with 0 and 45 degree direction angles and at 1 m and 2 m from the center of phantom (A-F, Figure 1) while the scatter radiation outside the room we observed at the distance of 30 cm, 1 m, and 2 m from glass door (G-I, Figure 1). All measurements with X2 survey probe were taken at 150 cm above the floor. Three dose reading were recorded to minimize random errors and then we calculated the average value of all the measurement.

The initial exposure technique was the clinical setting for the PA chest examination. The exposure index (EI) and deviation index (DI) values were used as an indicator of the amount of ionizing radiation on digital image receptor. The EI values are proportional to the signal to noise ratio squared and can be referred to image quality. These values provided useful feedback to radiographers when a digital image is overexposed or underexposed image.<sup>14,15</sup> In a study conducted by Lorusso showed that using a high tube voltage in range of 100-120 kVp is recommended to perform conventional portable chest radiography.<sup>16</sup> Exposure settings we used in PA projection of the thorax phantom ranging from 90 to 120 kVp with mAs adjustments for the glass barrier at 2.0-8.0 mAs. The appropriate exposure technique was selected from the scenario that getting closer to the target exposure index ( $EI_T$ ) diagnostic reference levels (Carestream  $EI_T=1751$ , Konica  $EI_T=355$ , using exposure at 5  $\mu\text{Gy}$ ) and to achieve a zero or minimize deviations from the index. The deviation index value was calculated by the following equation:  $DI=10 \log_{10} (EI/EI_T)$ . In conventional technique (leave the door open), the exposure range used 90-120 kVp and 2.0-3.2 mAs while imaging through the glass door was made for 90-120 kVp with adjusted mAs at 3.2-8.0 mAs. In this study, we have not considered in term of perceptual image quality, to only focus on optimizing technique parameters that reached image receptor and radiation dose in conventional portable chest radiography compared with through glass technique.

Lastly, we examined the effect of glass attenuation and changes in X-ray beam quality. The lower energy photons in the beam are generally absorbed or filtered out by the

glass. Therefore, we assessed the penetrating ability of X-ray beam before and after transmission through glass by measuring half-value layer (HVL). HVL measurements in term of equivalent thickness of aluminum in millimeters

(mm Al) at different X-ray tube voltages from 80 to 120 kVp. All data and statistical analysis were performed in Microsoft Excel for calculating descriptive statistics.

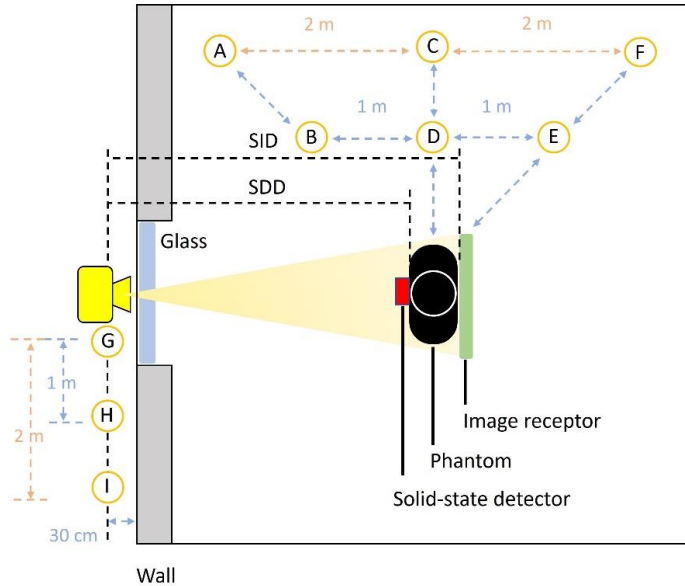


**Figure 1.** Experimental set-up with the locations marked. The anthropomorphic phantom was placed to acquire portable chest PA radiography at the source to image distance (SID) of 180 cm.



**Figure 2.** Positioning of the radiographic unit. Mobile x-ray machine was operated outside the room with door open (conventional technique) and through the glass barrier (TG-CXR technique) during image acquisition.



**Figure 3.** Setting up of the anthropomorphic phantom and the radiation dosimeter. (Left) A 152 cm-height of the anthropomorphic phantom was used for this experiment, and (Right) scatter measurement with X2 survey probe was taken at 150 cm above the floor.

## Results

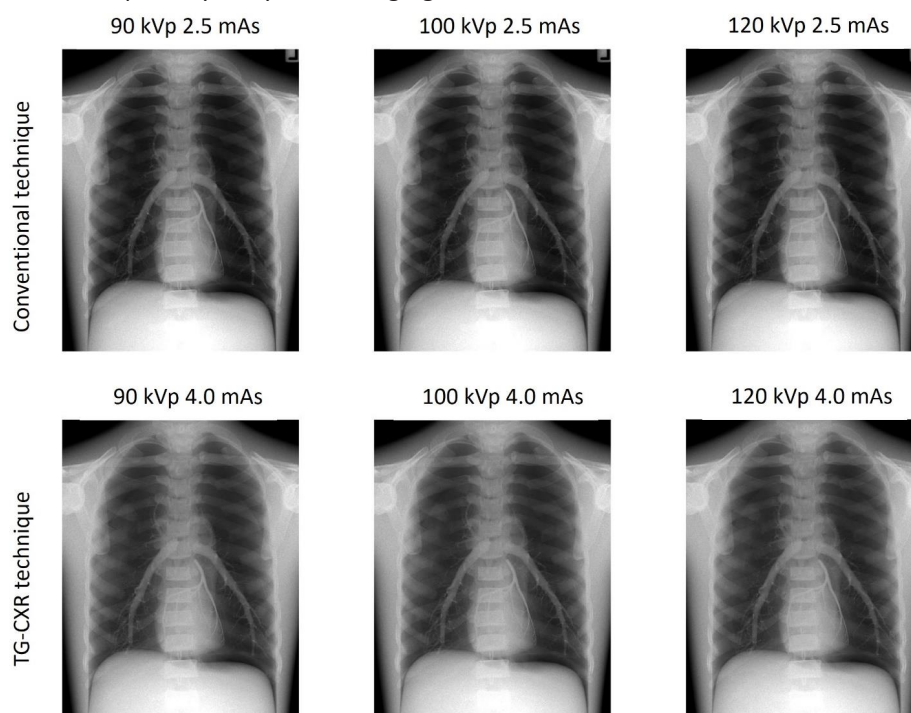
The results from the performance of each QC test showed that all are in the acceptable range within the AAPM Report No 93 and 74 recommendation. A total of 42 images were acquired using several exposure techniques without glass and through the glass barrier. Acquisition parameters are shown in Table 1 including the EI, DI, ESAK, % ESAK reduction, and %EI reduction. The range of EI and DI values were in the acceptable range for two CR imaging systems that provided a good image quality. Based on the fixed technique, the EI value with glass barrier was less than the EI value without glass. We found the average EI reduction on Carestream CR system was 10.4% while Konica Minolta was 37% with the glass barrier. ESAK reduction dropped by 56.6% in average (Table 1). In the conventional portable chest radiography (leave the door open), the appropriate exposure technique to generate a DI value closer to zero was 100 kVp with 2.5 mAs. This resulted in an average EI was 1742 for Carestream, 352.27 for Konica Minolta, and average ESAK was 46.73  $\mu\text{Gy}$ , respectively. To maintain a similar DI value to the conventional imaging with the glass barrier in the primary beam, the mAs adjustments were required to increase to 4.0 mAs. An increase of tube output needed by a factor of two (Figure 4-5). Overall, through glass portable chest radiography (TG-CXR technique) gave the average EI of 1795 for Carestream, 373.48 for Konica Minolta, and average ESAK was 30.52  $\mu\text{Gy}$ , respectively. Despite the increase of the mAs, the ESAK also decreased from 46.73  $\mu\text{Gy}$  without glass to 30.52  $\mu\text{Gy}$  with glass barrier. It was observed by the glass attenuates or filters some X-ray photon in the primary beam. Most of the beam hardening occurred when X-ray passed through the glass at 90 kVp.

Table 2 shows transmission measurement of the primary X-ray beam using normalized air kerma before and after transmission through glass. It can be seen from the data that the transmission of the primary X-ray beam ranging

from 35 to 44% at the range of 90-120 kVp. At higher tube voltage increased the average photon energy as the X-ray beam can penetrate more easily through matter. In other words, the intensity of the primary beam decreased with their ability to penetrate matter. For the transmission of the X-ray through glass barrier was decreased by nearly half of the initial beam intensity. A mean transmission of primary through glass barrier ranged from 35% to 44% at 90-120 kVp. Transmission measurement is consistent with the others reports.<sup>9</sup>

The results of scatter radiation measurement at the selected position for the same technique are shown in Table 3. Regarding to the position inside the room as shown in Figure 1, the side scatter and 45 degrees direction were observed over 1 or 2 meters away from the anthropomorphic phantom while the position outside the room corresponded to the radiographers stand when operating portable x-ray machine (standing close and standing far away). At the appropriate exposure technique of 100 kVp 2.5 mAs, the measured scatter air kerma were 0.08, 0.04, 0.03, 0.03 and 0.02  $\mu\text{Gy}/\text{mAs}$  at point A, B, C, D and E, respectively. Dosimeter recorded the scatter radiation at 30 cm from the glass door was 0.15  $\mu\text{Gy}/\text{mAs}$ . Scattered radiation dose reduced to 0.02  $\mu\text{Gy}/\text{mAs}$  at the radiographer standing 1-2 m away from the glass depending on the kVp used.

The HVL measurements of beam quality before and after transmission through glass are shown in Figure 6. At the X-ray tube voltage from 80 to 120 kVp, the HVL values of primary X-ray beam were 3.2 mm Al, 3.5 mm Al, 3.9 mm Al and 4.7 mm Al. The X-ray beam after transmission through glass resulted in the HVL of 5 mm Al at 80 kVp, 5.5 mm Al at 90 kVp, 6.1 mm Al at 100 kVp and 7.1 mm Al at 120 kVp respectively. The HVL increased from 3.9 to 6.1 mm Al indicating the effect of beam hardening by plain glass.



**Figure 4.** Examples of chest radiographs from Konica Minolta CR system. Images obtained by conventional radiography and through the glass technique using the fixed mAs at the range of 90, 100, and 120 kVp, respectively (from left to right).

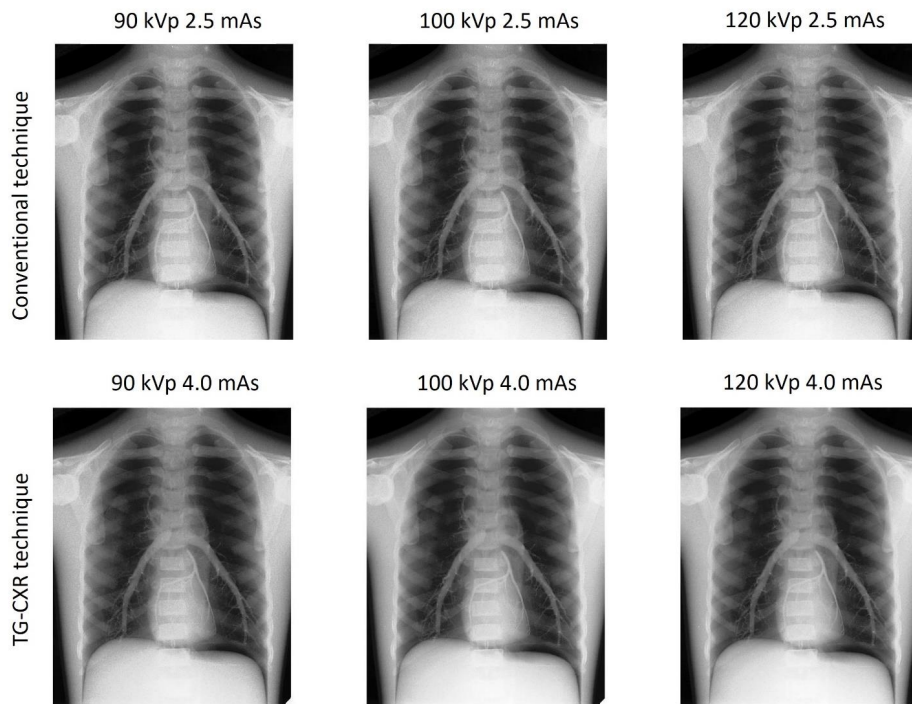


Figure 5. Examples of chest radiographs from Carestream CR system. Images obtained by conventional radiography and through the glass technique using the fixed mAs at the range of 90, 100, and 120 kVp, respectively (from left to right).

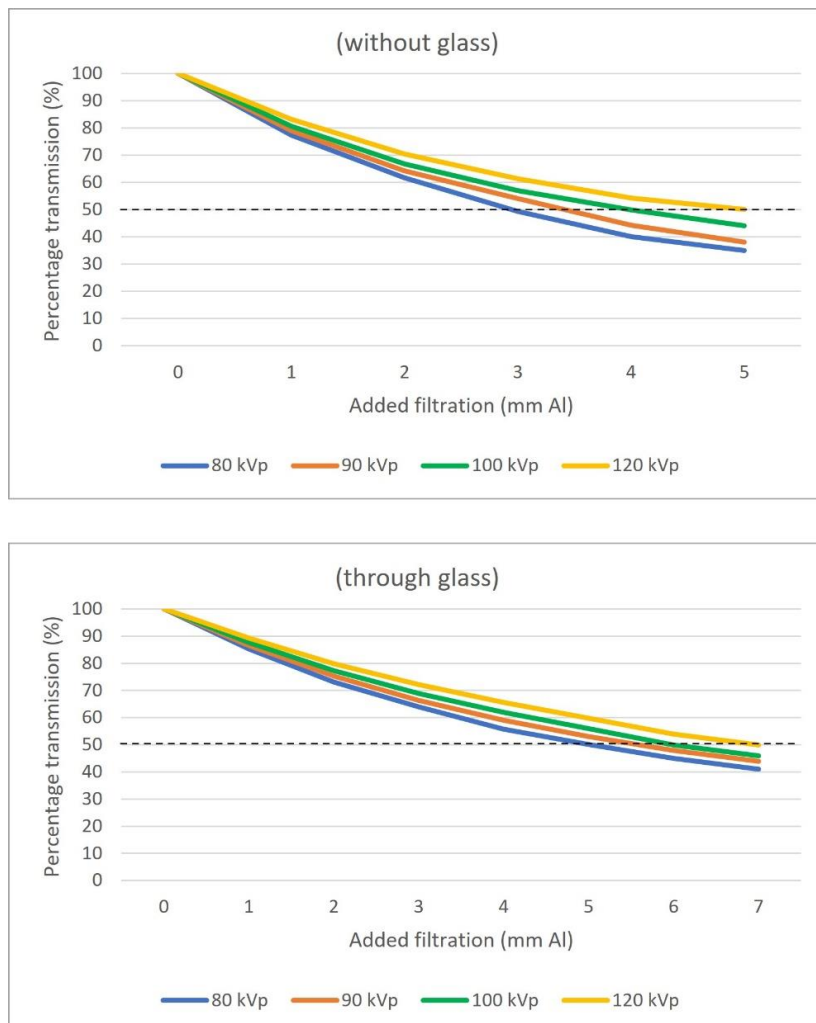


Figure 6. Comparison of half-value layer (HVL) and percentage of X-ray beam before and after transmission through glass barrier. One mm of aluminum sheet was used for the X-ray tube voltage 80-120 kVp. Dotted line represents the amount or thickness of aluminum required to reduce the x-ray beam to half of its original intensity.

**Table 1** Summary of the exposure technique setting for portable chest radiography, the range of EI and DI values from two imaging CR systems, and entrance surface air kerma measurements with and without the glass barrier.

Chest PA	kVp	mAs	EI	EI	DI	DI	ESAK ( $\mu\text{Gy}$ )	% ESAK reduction	% EI reduction				
			Carestream	Konica	Carestream	Konica			Carestream	Konica			
Conventional technique	90	2.0	1391	187.27	-0.99	-2.78	29.30	60.5	10.6	36.8			
		2.5	1568	251.41	-0.47	-1.50	38.03						
		3.2	1724	330.03	-0.07	-0.31	49.75						
	100	2.0	1668	279.44	-0.06	-1.04	36.49						
		2.5	1742	352.27	-0.02	-0.03	46.73						
		3.2	1884	474.01	0.32	1.25	60.52						
	120	2.0	1852	452.14	0.24	1.05	50.48						
		2.5	1987	567.43	0.55	2.03	65.07						
		3.2	2100	784.40	0.79	3.44	84.45						
TG-CXR Technique	90	3.2	1541	208.61	-0.55	-2.31	19.67	57.0	10.8	38.8			
		4.0	1612	257.71	-0.36	-1.39	23.75						
		6.3	1775	376.01	0.06	0.25	27.80						
		8.0	1923	510.52	0.41	1.58	36.10						
	100	3.2	1680	290.15	-0.18	-0.88	26.02						
		4.0	1795	373.48	0.11	0.22	30.52						
		6.3	1928	537.62	0.41	1.80	35.98						
		8.0	2072	739.85	0.73	3.19	41.80						
	120	3.2	1896	507.09	0.34	1.55	40.30				52.3	9.7	35.4
		4.0	2065	761.80	0.72	3.32	47.11						
		5.0	2107	814.97	0.80	3.61	55.72						
		6.3	2178	945.02	0.94	4.25	64.30						

kVp, peak kilovoltage; mAs, milliampere seconds; EI, Exposure index; DI, Deviation index; ESAK, Entrance surface air kerma. A positive or negative DI indicates the amount of exposure greater or lesser than the target EI.

**Table 2** Transmission measurement of normalized air kerma before and after glass barrier.

kVp	Air kerma ( $\mu\text{Gy}/\text{mAs}$ )		Percentage transmission (%)
	Before glass barrier	After glass barrier	
90	15.14 $\pm$ 0.45	5.25 $\pm$ 0.92	35
100	18.62 $\pm$ 0.34	6.67 $\pm$ 1.42	36
120	25.89 $\pm$ 0.59	11.43 $\pm$ 1.01	44

**Table 3** Normalized scatter air kerma measurement with tube voltages ranging from 90 to 120 kVp, in 10 kVp increments, for through glass technique at the selected position during image acquisition inside the room (from phantom) and outside the room (from glass barrier).

Tube voltage	Scatter air kerma ( $\mu\text{Gy} / \text{mAs}$ ) inside the room								
	A	B	C	D	E	F	G	H	I
90	0.07 $\pm$ 0.02	0.03 $\pm$ 0.02	0.02 $\pm$ 0.02	0.02 $\pm$ 0.01	0.02 $\pm$ 0.02	0.01 $\pm$ 0.01	0.11 $\pm$ 0.01	0.01 $\pm$ 0.01	0.01 $\pm$ 0.01
100	0.08 $\pm$ 0.03	0.04 $\pm$ 0.01	0.03 $\pm$ 0.01	0.03 $\pm$ 0.02	0.03 $\pm$ 0.01	0.02 $\pm$ 0.02	0.15 $\pm$ 0.02	0.02 $\pm$ 0.02	0.02 $\pm$ 0.01
120	0.10 $\pm$ 0.03	0.04 $\pm$ 0.01	0.03 $\pm$ 0.01	0.04 $\pm$ 0.03	0.03 $\pm$ 0.01	0.03 $\pm$ 0.03	0.22 $\pm$ 0.02	0.02 $\pm$ 0.01	0.02 $\pm$ 0.01

## Discussion

With an increase in radiology workload for staff during the COVID-19 Pandemic, through glass portable chest radiography technique is useful to radiographers and help to reduce the risk of infection. TG-CXR technique has allowed to prevent infection in the hospital setting, less personal protective equipment (PPE) use, decreased radiography equipment sanitization, and limit staffs' exposure to the virus that make them feel safe. Moreover, it notably allows for net operating costs per annum to be reduced for several reasons with those observed by Liu *et al.*<sup>17</sup> This is compared with standard portable or bedside radiography by a team of two radiographers for these patients in the hospital ward.

As to the results obtained in this study, images obtained by through glass portable radiography were satisfied with high kVp technique and variable mAs to control the image quality and patient dose. These results seem to be consistent with earlier studies which found the radiographic exposure technique of TG-CXR ranging from 100-125 kVp at 4.5-12.0 mAs. These values vary depending on source to image distance and patient variables of small, medium, and large body size.<sup>8-11</sup> However, the EI values from two CR systems were found within the range recommended by the manufacturer. Using the fixed kVp and mAs exposure settings, images obtained with TG-CXR technique showed lower EI value than conventional technique. This resulted in a slightly grainy appearance (quantum mottle) on the image due to low signal-to-noise ratio (SNR). Low SNR reduced spatial resolution and thus provided of image quality degradation. This implies that selection of appropriate exposure technique is still needed to produce a clinically acceptable image and safety of patients undergoing radiographic examinations. Our findings suggest that double mAs is also needed to produce good diagnostic image for modified through glass imaging. The attenuation and HVL with and without glass were similar to those observed by others.<sup>9, 18, 19</sup>

Based on clinical setting, the higher kVp used in radiological procedure, the better penetrating of X-ray beam is provided. This resulted in lower radiation dose to patient. For portable radiography, or bedside chest radiograph, at the radiographer standing distance of 1-2 m away from the glass, scattered radiation dose reduced to 0.02  $\mu$ Gy/mAs. It is apparent that scatter radiation from X-ray transmission through the glass barrier was low. Similar findings were noted by Brady *et al.*<sup>9</sup> who suggested the minimum distance of 1 metre from radiation source was equal to the dose from natural background radiation around three hours. In fact, radiographers stand when operating the exam more than a metre away could be even lower. This low-level exposure to radiation was generally considered safe to use.<sup>18, 20, 21</sup>

As we known the COVID-19 pandemic has a global impact across the world. In support of Cho et al. observed that the number of radiology examinations decreased during the pandemic, longer turnaround time required for portable radiography in COVID-19 patients, extended period of time for donning personal protective equipment in the examination of these patients.<sup>21</sup> One the other hand, we found that many attempts have been made in order to enhance portable chest radiography in response to the pandemic. Le *et al.*<sup>22</sup> have

developed deep neuron network to enhance the speed and diagnostic accuracy for COVID-19 patient. They found the performance of the proposed method improved image contrast between masses and normal lung, better costophrenic angles perception, and improved conspicuity of opacities in lower lobes which is a feature of COVID-19. Comparison of these finding with those of other studies confirms deep learning artificial intelligence methods have a significant opportunity to contribute diagnostic accuracy and efficiency.<sup>23-26</sup>

Our experiments were based on anthropomorphic phantom exposure and one type of mobile X-ray unit. In the clinical setting they are much more situations will be involved rather than simulated clinical scenario we made. These techniques will likely be applicable to other airborne infectious diseases and applied to any parts of the body in radiographic examinations. Only one type of glass and 5 mm thickness were tested. Considerably more work in different type of glass, different glass materials, different size and thicknesses will need to be developed. However, it is also important to note that the isolation room of COVID-19 patient needs to have a clear glass door or window size which is large enough to set-up mobile X-ray unit and equipment without any obstruction in the path of the primary X-ray beam. TG-CXR technique required specific room design or modified room construction that will not be available for all hospitals. Again, this study did not compare image quality between conventional and through glass portable radiography in term of image quality metrics (e.g., SNR, CNR, spatial resolution, sharpness, and the noise level). Further study of image quality assessment between these two are warranted.

## Conclusion

Through glass portable radiography technique are feasible and safe. Radiographers can avoid prolonged close contact with COVID-19 patients during their work. The appropriate exposure technique for conventional portable chest computed radiography of anthropomorphic phantom was 100 kVp and 2.5 mAs at SID of 180 cm. When modified X-ray imaging through glass barrier, double mAs is also needed to produce good diagnostic image (100 kVp and 4.0 mAs). X-ray beam after transmission through glass thickness 5 mm was 36% and the HVL of beam increased from 3.9 to 6.1 mm Al indicating the effect of beam hardening by glass. Scatter inside and outside the room could be observed at low dose levels.

## Acknowledgements

The author received no financial support for the research. The author also would like to express my sincere gratitude to the Department of Radiological Technology, Faculty of Allied Health Sciences, Naresuan University for all supporting facilities.

## Conflict of interest

The author declares no conflicts of interest in this research.

## References

- [1] Mossa-Basha M, Medverd J, Linnau KF, Lynch JB, Wener MH, Kicska G, et al. Policies and guidelines for COVID-19 preparedness: experiences from the University of Washington. *Radiology*. 2020; 296(2): E26-E31.
- [2] Goyal A, Tiwari R, Bagarhatta M, Ashwini B, Rath B, Bhandari S. Role of portable chest radiography in management of COVID-19: Experience of 422 patients from a tertiary care center in India. *Indian J Radiol Imaging*. 2021;31(Suppl 1): S94.
- [3] Chamorro EM, Tascón AD, Sanz LI, Vélez SO, Nacenta SB. Radiologic diagnosis of patients with COVID-19. *Radiología (English Edition)*. 2021; 63(1): 56-73.
- [4] Jacobi A, Chung M, Bernheim A, Eber C. Portable chest X-ray in coronavirus disease-19 (COVID-19): A pictorial review. *Clinical imaging*. 2020; 64: 35-42.
- [5] Jain A, Patankar S, Kale S, Bairy A. Imaging of coronavirus disease (COVID-19): A pictorial review. *Pol J Radiol*. 2021; 86: e4-e18. doi: 10.5114/pjr.2021.102609.
- [6] Akudjedu TN, Mishio NA, Elshami W, Culp MP, Lawal O, Botwe BO, et al. The global impact of the COVID-19 pandemic on clinical radiography practice: A systematic literature review and recommendations for future services planning. *Radiography*. 2021; 27(4): 1219-26.
- [7] Niu Y, Xian J, Lei Z, Liu X, Sun Q. Management of infection control and radiological protection in diagnostic radiology examination of COVID-19 cases. *Radiat Med Prot*. 2020;1(02): 75-80.
- [8] Moirano JM, Dunnam JS, Zamora DA, Robinson JD, Medverd JR, Kanal KM. Through-the-glass portable radiography of patients in isolation units: Experience during the COVID-19 pandemic. *AJR Am J Roentgenol*. 2021; 217(4): 883-7.
- [9] Brady Z, Scoullar H, Grinsted B, Ewert K, Kavnoudias H, Jarema A, et al. Technique, radiation safety and image quality for chest X-ray imaging through glass and in mobile settings during the COVID-19 pandemic. *Physical and engineering sciences in medicine*. 2020; 43(3): 765-79.
- [10] Gange CP, Pahade JK, Cortopassi I, Bader AS, Bokhari J, Hoerner M, et al. Social distancing with portable chest radiographs during the COVID-19 pandemic: Assessment of radiograph technique and image quality obtained at 6 feet and through glass. *Radiol: Cardiothoracic Imaging*. 2020; 2(6): e200420. doi: 10.1148/ryct.2020200420.
- [11] Sng LH, Arlany L, Toh LC, Loo T, Ilzam N, Wong B, et al. Initial data from an experiment to implement a safe procedure to perform PA erect chest radiographs for COVID-19 patients with a mobile radiographic system in a "clean" zone of the hospital ward. *Radiography*. 2021; 27(1): 48-53.
- [12] Medicine AAoPi. Quality control in diagnostic radiology. *AAPM Report*. 2002; 74.
- [13] Seibert JA, Bogucki TM, Ciona T, Huda W, Karellas A, Mercier J, et al. Acceptance testing and quality control of photostimulable storage phosphor imaging systems. *Rpt of AAPM Task Group*. 2006(10).
- [14] Dave JK, Jones AK, Fisher R, Hulme K, Rill L, Zamora D, et al. Current state of practice regarding digital radiography exposure indicators and deviation indices: Report of AAPM Imaging Physics Committee Task Group 232. *Medical physics*. 2018; 45(11): e1146-e60.
- [15] Protection ICoR. Diagnostic reference levels in medical imaging: review and additional advice. *Ann ICRP*. 2001; 31(4): 33-52.
- [16] Lorusso JR, Fitzgeorge L, Lorusso D, Lorusso E. Examining Practitioners' Assessments of perceived aesthetic and diagnostic quality of high kVp–low mAs pelvis, chest, skull, and hand phantom radiographs. *J Med imaging Radiation Sci*. 2015; 46(2): 162-73.
- [17] Liu TY, Rai A, Ditkofsky N, Deva DP, Dowdell TR, Ackery AD, et al. Cost benefit analysis of portable chest radiography through glass: Initial experience at a tertiary care centre during COVID-19 pandemic. *J Medical Imaging Radiat Sci*. 2021; 52(2): 186-90. doi: 10.1016/j.jmir.2021.30.036.
- [18] McKenney SE, Wait JM, Cooper III VN, Johnson AM, Wang J, Leung AN, et al. Multi-institution consensus paper for acquisition of portable chest radiographs through glass barriers. *J App Clin Med P hys* 2021; 22(8): 219-29.
- [19] Chan J, Auffermann W, Jenkins P, Streitmatter S, Duong P-A. Implementing a novel through-glass chest radiography technique for COVID-19 patients: image quality, radiation dose optimization, and practical considerations. *Curr Probl Diagn Radiology*. 2022; 51(1): 38-45.
- [20] Rai A, MacGregor K, Hunt B, Gontar A, Ditkofsky N, Deva D, et al. Proof of concept: phantom study to ensure quality and safety of portable chest radiography through glass during the COVID-19 pandemic. *Investig radiol*. 2021; 56(3): 135-40.
- [21] Cho J, Lee S, Gu BS, Jung SH, Kim HY. The Impact of COVID-19 on the use of radiology resources in a tertiary hospital. *J Korean Med Sci*. 2020; 35(40): e368. doi: 10.3346/jkms.2020.35. e368.!
- [22] Le N, Sorensen J, Bui T, Choudhary A, Luu K, Nguyen H. Enhance portable radiograph for fast and high accurate COVID-19 monitoring. *Diagnostics*. 2021; 11(6): 1080.
- [23] Hussain L, Nguyen T, Li H, Abbasi AA, Lone KJ, Zhao Z, et al. Machine-learning classification of texture features of portable chest X-ray accurately classifies COVID-19 lung infection. *BioMed Eng OnLine*. 2020; 19(1): 1-18.

- [24] Kikkiseti S, Zhu J, Shen B, Li H, Duong TQ. Deep-learning convolutional neural networks with transfer learning accurately classify COVID-19 lung infection on portable chest radiographs. *PeerJ*. 2020; 8: e10309.
- [25] Basu S, Mitra S, Saha N, editors. Deep learning for screening covid-19 using chest x-ray images. 2020 IEEE Symposium Series on Computational Intelligence (SSCI); 2020: IEEE.
- [26] Zhu J, Shen B, Abbasi A, Hoshmand-Kochi M, Li H, Duong TQ. Deep transfer learning artificial intelligence accurately stages COVID-19 lung disease severity on portable chest radiographs. *PLoS One*. 2020; 15(7): e0236621.